Potential-invariant network structures in Asakura-Oosawa mixtures with very short attraction range

Potential-invariant network structures in Asakura-Oosawa mixtures with very short attraction range

Fernando Soto-Bustamante,[1] Néstor E. Valádez-Pérez,[2] Ramón Castañeda-Priego,[1] and Marco Laurati[3, a)]
[1)] *División de Ciencias e Ingenierías, Universidad de Guanajuato, Lomas del Bosque 103, 37150 León, Mexico*
[2)] *Facultad de Ciencias en Física y Matemáticas, Universidad Autónoma de Chiapas, Carretera Emiliano Zapata km 8, 29050, Tuxtla Gutiérrez, Chiapas, Mexico*
[3)] *Dipartimento di Chimica and CSGI, Università di Firenze, 50019 Sesto Fiorentino, Italy.*

(Dated: 23 June 2021)

We systematically investigated the structure and aggregate morphology of gel networks formed by colloid-polymer mixtures with moderate colloid volume fraction and different values of the polymer-colloid size ratio, always in the limit of short-range attraction. Using the coordinates obtained from confocal microscopy experiments, we determined the radial, angular and nearest-neighbor distribution functions together with the cluster radius of gyration as a function of size ratio and polymer concentration. The analysis of the structural correlations reveals that the network structure becomes increasingly less sensitive to the potential strength with decreasing the polymer-colloid size ratio. For the larger size ratios compact clusters are formed at the onset of network formation and become progressively more branched and elongated with increasing polymer concentration/attraction strength. For the smallest size ratios, we observe that the aggregate structures forming the gel network are characterized by similar morphological parameters for different values of the size ratio and of the polymer concentration, indicating a limited evolution of the gel structure with variations of the parameters that determine the interaction potential between colloids.

I. INTRODUCTION

Colloidal suspensions are of primary importance for industrial applications in paints, food, pharmaceuticals, cosmetics, among others[1–4]. In the presence of attractive interactions colloidal aggregation is observed, with important consequences for the stability of suspensions[5] and shelf-life, and for degenerative diseases associated with proteins[6–8]. Fundamental understanding on aggregation phenomena has been achieved through model systems, in particular mixtures of hard-sphere colloids and non-adsorbing polymers, typically known as Asakura-Oosawa mixtures[9,10], in which the range and strength of the attractive interaction can be carefully controlled through the polymer-colloid size ratio and polymer concentration[11,12]. The effective forces between colloids induced by the polymer, also called depletion forces, have been associated to physical mechanisms in important thermodynamic processes in and out of thermodynamic equilibrium. For example, state diagrams obtained as a function of polymer concentration and colloid volume fraction revealed cluster and gel formation[13–21].

For hard-core repulsion and short range attraction, i.e. polymer-colloid size ratios < 0.1, a condition for which interactions are often modeled by means of the Aasakura-Oosawa potential[22], cluster formation is observed as a precursor of gelation[23–25], which is driven by arrested phase separation. If in addition a competing long range repulsion is present, typically associated with electrostatic interactions, changes in phase behavior occur[26] and stabilization of cluster fluids at low colloidal packing fractions is observed[16,27–30]. Furthermore the long range repulsion affects the route leading to gelation[31–33] and the gel structure[34–36], with important consequences on mechanical properties[37,38]. Previous studies investigated the connection between the parameters controlling the attractive component of the potential and the microstructure of aggregates, showing that the range[39–43] and strength[17,44,45] influence cluster morphology and growth. Recent findings indicate that the combined effect of the range and strength of attraction, represented in the form of the second virial coefficient, determines the fractal dimension of the reversible aggregates[46]. These studies mainly investigated the morphology of aggregates in cluster fluids[44–46], or when investigating gel structures mainly focused on the effects of one control parameter[17].

In this contribution, we present a detailed experimental analysis of cluster morphology in non-equilibrium gel structures formed by low volume fraction colloid-polymer mixtures with short-range attractive interactions and weak long-range repulsion. We focus on the effects of the control parameters of the attractive component and show that while for larger values of the attraction range the cluster morphology is dependent on both strength and range of the interaction, the dependence becomes increasingly less pronounced for smaller polymer-colloid size ratios, until the network structure becomes essentially invariant on both parameters.

II. MATERIALS AND METHODS

A. Samples

We investigated mixtures of Polymethylmethacrylate (PMMA) hard sphere-like particles and non-adsorbing polystyrene (PS) chains dispersed in a solvent composed of cis-trans decahydronaphtalene and bromocycloheptane (CHB) that matches the density of the PMMA particles. The

[a)] Electronic mail: marco.laurati@unifi.it

particles are sterically stabilized by a layer of grafted polyhydroxystearic acid (PHSA). Their diameter is $\sigma \equiv 2R$ = 1.7μm, as determined by dynamic light scattering (DLS). The particles are fluorescently labeled with nitrobenzoxadyazole (NBD). PS chains with molecular weight $M_w = 3\cdot10^6$, $1.01\cdot10^6$, $8.64\cdot10^5$, $4.51\cdot10^5$, $1.01\cdot10^5$ were used. The corresponding radius of gyration r_g was obtained using the following empirical relation which has been determined by DLS measurements of dilute solutions of PS in cis-decalin[47]:

$$r_g = r_g^\theta \sqrt{1+\frac{134}{105}z(T)}, \quad (1)$$

where $r_g^\theta = 0.0276\sqrt{M_w}$ is the radius of gyration at the θ temperature T_θ and $z(T)$ is the Fixman parameter[47]:

$$z(T) = 0.00975\sqrt{M_w}(1-\frac{T_\theta}{T}). \quad (2)$$

We have neglected any small swelling effect induced by the presence of CHB in addition to decalin in our samples. Values of r_g and of the polymer colloid size-ratio $\xi = r_g/R$ for the different polymers used are reported in Table I. The suspensions present a certain degree of charging. A precise determination of the electrostatic contribution to the interaction potential is complicated because the ionic strength of CHB varies from batch to batch and also as a function of time (see Ref.[48]). However, assuming the largest value of the charge $Z \sim 500$ found in literature, we could estimate a thickness of the double layer, namely, $\kappa^{-1} \sim 0.84\sigma$, where κ is the so-called screening parameter[49]; this estimation is based on a Poisson-Boltzmann approach assuming that the effective charge at saturation has been reached ($Z_{\rm eff}^{\rm sat} \sim 50$)[49]. This value is slightly smaller than that reported in previous studies.[32,48,50] The obtained screening parameter, $\kappa\sigma > 1$, thus indicates that the electrostatic contribution is weak and decays rapidly beyond a particle diameter. Therefore, the system is mainly dominated by the short-range attraction. The weakness of the electrostatic contribution is also supported by the fact that suspensions without polymers investigated in this work were crystallizing into FCC lattices at $\phi \approx 0.47$[50]. The values of r_g were used to calculate the overlap concentration $c_p^* = 3M_w/4\pi N_A r_g^3$. Samples with colloidal volume fraction $\phi = 0.10$ and values of $c_p/c_p^* = 0.05$, 0.10, 0.20, 0.30, 0.40, 0.50, 0.75, 1.00 were prepared by mixing proper amounts of colloid and polymer stock solutions. Before measurement, samples were mixed in a vortex and homogeneized for 24 hours in a rotating wheel.

B. Confocal Microscopy

For each sample, 50 stacks of 151 images of 512x512 pixels, corresponding to a volume of 58x58x30 μm^3 were acquired using a VT-Eye (Visitech) Confocal Unit mounted on a Nikon Ti-S inverted microscope. A 100x Nikon Plan APO VC oil-immersion objective with N.A. = 1.40 was used to acquire the images. Each stack was measured at a distance of 10 μm from the coverslip in order to avoid any effect on the structure due to the vicinity of a surface. Particle coordinates were extracted from image stacks using standard particle tracking routines[51].

TABLE I. Values of the radius of gyration r_g and corresponding polymer-colloid size ratio ξ for the linear PS chains used in this work.† Values provided by the producer (Polymer Source inc.).

$M_w^\dagger$ [g·mol^{-1}]	r_g [μm]	ξ
$3.00\cdot10^6$	0.0636	0.075
$1.01\cdot10^6$	0.0333	0.039
$8.64\cdot10^5$	0.0305	0.036
$4.51\cdot10^5$	0.0211	0.025
$1.01\cdot10^5$	0.0093	0.011

III. RESULTS AND DISCUSSION

A. Cluster morphology as a function of depletant concentration

We consider in this section colloid-polymer mixtures for two specific colloid-polymer size ratios, $\xi = 0.075$ and 0.011, and different values of polymer concentration. These values of ξ correspond to the limits of the range of investigated size ratios and were chosen in order to highlight the maximal differences between changes induced by depletant concentration for different values of ξ. The effects of the entire range of ξ values on aggregate structure will be discussed in detail in the following section. We report in Fig.1 the radial distribution function:

$$g(r) = \frac{N(r)}{4\pi n r^2 \Delta r}, \quad (3)$$

which was determined from particle coordinates extracted from confocal microscopy experiments, with $N(r)$ the number of particles in a thin shell of thickness Δr at distance r from a selected particle and n the total particle number density. For $\xi = 0.075$ (Fig.1a, top), and small polymer concentrations ($c_p/c_p^* = 0.05$, 0.10, 0.20), the $g(r)$ shows a small first peak at a distance $r_{\rm peak} \approx 2.2\mu$m and a very small second peak at about $2r_{\rm peak}$, indicative of a fluid structure. This is confirmed by the snapshots in the inset of Fig.1a which evidence a uniform distribution of particles. For $c_p/c_p^* = 0.10$ a peak at a distance $r \approx 1.7\mu$m is additionally observed, indicating the presence of a certain amount of particles in contact. For $c_p/c_p^* = 0.30$ the $g(r)$ indicates a pronounced structural change: The first peak is now observed for $r_{\rm peak} \approx 1.7\mu$m and presents a height of about 10, indicating the formation of a large number of particle contacts. The second peak also moves to a smaller distance, $r_{\rm 2peak} \approx 3.2\mu$m, which is slightly smaller than $2r_{\rm peak}$. The second peak is split, indicating a densely packed second shell of nearest neighbors, typical of globular aggregates. The $g(r)$ thus indicates the presence of compact cluster structures, as confirmed by the snapshot of the sample in Fig.1a (top). Moreover, 3D renderings of sample volumes show the presence of a percolated space spanning

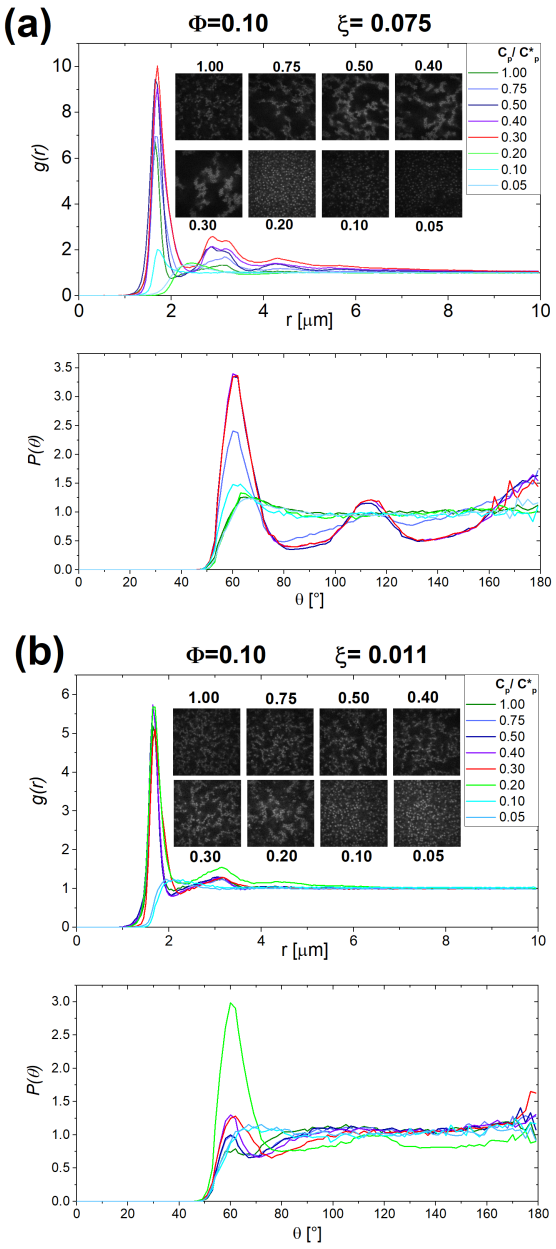

FIG. 1. Radial (top) and angular (bottom) distribution functions, $g(r)$ and $P(\theta)$, of samples with $\phi = 0.10$ and different polymer concentrations c_p/c_p^*, as indicated, for (a) $\xi = 0.075$ and (b) $\xi = 0.011$. Insets: 2D images of the samples obtained by confocal microscopy.

network (see Suppl. Material). Increasing further c_p/c_p^* the peaks of the $g(r)$ progressively decrease and the first minimum shifts to smaller distances. In addition, the splitting of the second peak becomes less pronounced and disappears for $c_p/c_p^* = 0.75$ and 1.00. For these samples the second peak is also particularly broad and flat: The snapshots of the samples evidence elongated and branched cluster structures (Fig.1a, top). Therefore, while compact cluster structures are formed at the onset of gelation, there is a progressive transition to more elongated aggregate structures with increasing c_p/c_p^*.

A similar structural transition has been observed in colloid-polymer mixtures with larger colloid volume fraction[17]. The evolution from compact to elongated aggregate structures with increasing polymer concentration/attraction strength can be understood with the following qualitative argument: For moderate attractions, a small local particle mobility allowed by the range of the potential makes the bond flexible. This allows bond reorientation to accommodate additional particles and leads to more compact aggregates. When the attraction increases, the bonds become rigid, and reorientation is suppressed, favoring the formation of more elongated and branched structures. The transition is confirmed by the bond angular distribution functions $P(\theta)$ reported in Fig.1a (bottom). This distribution takes into account trios of bonded particles, i, j and k, and θ is the angle between vectors $\mathbf{r}_j - \mathbf{r}_i$ and $\mathbf{r}_k - \mathbf{r}_i$. The distribution reported here is the normalized one given in reference[52] as

$$\frac{1}{\pi}\int_0^\pi \frac{P(\theta)}{\sin\theta} d\theta = 1. \qquad (4)$$

$P(\theta)$ gives information about the local arrangement of particles in a cluster without referring to any particular direction. Compact, triangular arrangements correspond to $\theta = 60°$, more open configurations correspond to larger θ values.

For the smallest values of c_p/c_p^*, $P(\theta)$ is almost flat; for intermediate values (c_p/c_p^* = 0.30, 0.40, 0.50) it shows peaks at multiples of 60°, which indicate triangular structures typical of compact clusters. Instead, for larger values of c_p/c_p^* the first peak around 60° is less pronounced, the second peak moves to smaller angular values, around 100°, and becomes also flatter, indicating formation of more elongated and less compact structures. If we now consider the analogue samples with $\xi = 0.011$, the $g(r)$ of $c_p/c_p^* = 0.05$ and 0.10 are similar to those of the corresponding samples with $\xi = 0.075$ (Fig.1b, top). However, at $c_p/c_p^* = 0.20$ formation of aggregates is already indicated by the shift of the first peak position to $r_{\text{peak}} \approx 1.7\mu$m and by its larger height. The 3D rendering of the structure also evidences formation of a percolated network (see Suppl. Material). However, the shape of this $g(r)$ is rather similar to that of samples with $\xi = 0.075$ and $c_p/c_p^* = 0.75$ and 1.00. Note also that the difference between the $g(r)$ for $c_p/c_p^* = 0.20$ and those for larger values of the polymer concentration is very moderate. The snapshots of the samples in Fig. 1b (top) confirm that a network structure of elongated clusters is directly formed at $c_p/c_p^* = 0.20$ and that the clusters only become slightly thinner with increasing c_p/c_p^*. This limited dependence of the network structure on the polymer concentration is confirmed by the angular distribution functions of Fig.1b (bottom): only the sample with $c_p/c_p^* = 0.20$ shows some indication of the formation of more compact clusters, while all other samples show similar $P(\theta)$ indicating elongated aggregates. The suppression of the formation of compact clusters is due to the fact that for this short range of attraction, the strength of the potential in the gel state is always large enough to immobilize bonded particles and favor the formation of elongated structures.

The neighbor distribution $P(n_b)$ (Fig.2a) for samples with $\xi = 0.075$ confirms the structural evolution of clusters indi-

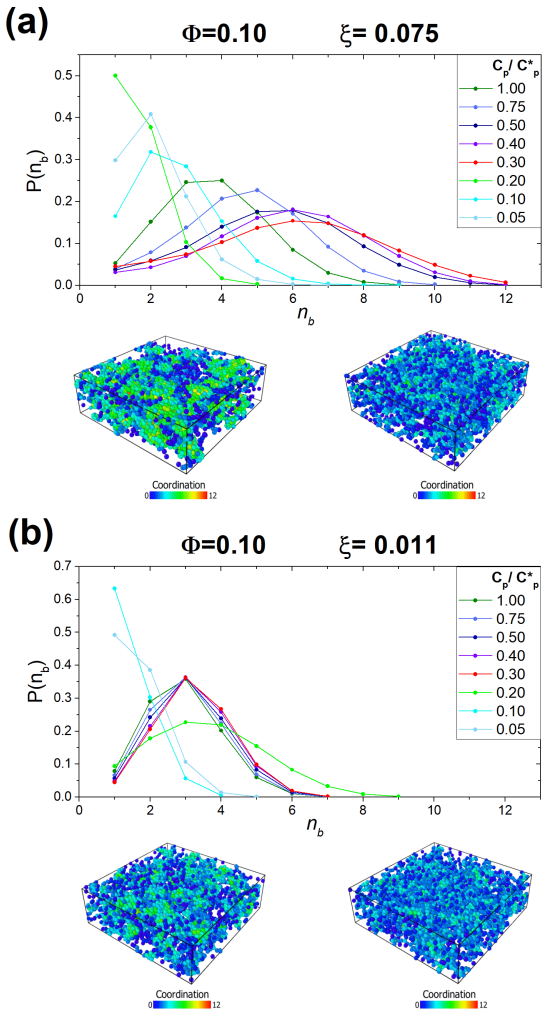

FIG. 2. Nearest neighbor (n_b) distribution function $P(n_b)$ of samples with $\phi = 0.10$ and different polymer concentrations c_p/c_p^*, as indicated for (a) $\xi = 0.075$ and (b) $\xi = 0.011$. Bottom: Renderings of volumes corresponding to samples with (a) c_p/c_p^* = 0.30 (left), and 1.00 (right). (b) c_p/c_p^* = 0.20 (left), and 1.00 (right). Particle color scale represents the number of neighbors (coordination).

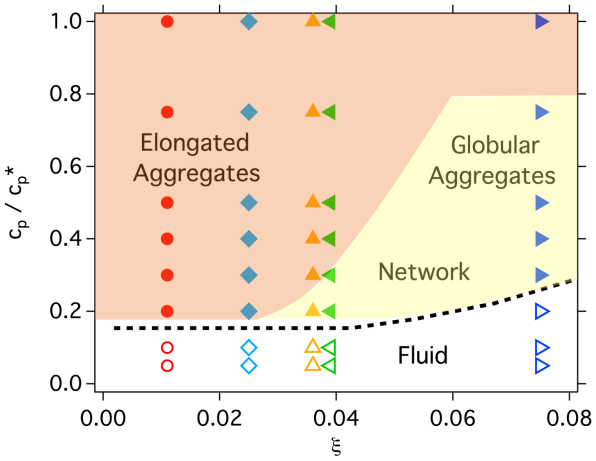

FIG. 3. State diagram indicating fluid (open symbols) and percolated gel states (full symbols) for all investigated size ratios ξ and polymer concentrations c_p/c_p^*. The dashed line represents the estimated percolation line. Regions of more elongated or more globular aggregate structures are indicated by the shaded areas.

cated by $P(\theta)$: it is centered around $n_b = 2$ neighbors for the smallest values of c_p/c_p^* and relatively narrow. Note that two particles were considered as being neighbors when the distance between their centers was smaller than $2R + 2r_g$, a criterion which corresponds to considering two particles forming a bond when they lie within the range of the attractive interaction induced by depletion forces. Moderate variations of this choice of the cutoff quantitatively change the distributions but do not alter their shape. The distribution is centered around $n_b = 6$ for $c_p/c_p^* = 0.30$, 0.40 and 0.50, being maximally broad for $c_p/c_p^* = 0.30$. It is centered around $n_b = 5$ for $c_p/c_p^* = 0.75$ and finally the center moves back to 4 for $c_p/c_p^* = 1.00$. For the last two values the distribution is again narrower. The renderings of the samples obtained from coordinates extracted from confocal microscopy experiments (Fig.2a, bottom) show that the broadest distribution observed for $c_p/c_p^* = 0.30$ corresponds to a more pronounced structural heterogeneity. For $\xi = 0.011$ (Fig.2b) instead all distributions of samples with $c_p/c_p^* \geq 0.20$ are centered around $n_b = 3$, with only the one for $c_p/c_p^* = 0.20$ being broader. The renderings also show a moderate change in the degree of heterogeneity of the network structures (Fig.2b, bottom).

In summary, the analysis of different distribution functions characterizing the structure of mixtures at the largest and smallest polymer-colloid size ratio ξ investigated show that while the samples with $\xi = 0.075$ present a significant structural evolution as a function of c_p/c_p^*, with formation of more compact clusters at small values of c_p/c_p^* and more open, branched structures at large values of c_p/c_p^*, samples with $\xi = 0.011$ are much less sensitive to the value of c_p/c_p^* and directly form networks of elongated aggregates.

B. Effect of depletant size

Fig.3 reports the state diagram of the system for different values of the size ratio ξ, in which fluid and percolated network (gel states) were distinguished. Networks/Gel states were distinguished from fluids based on the presence of a space spanning network in the 3D reconstructions obtained from the coordinates extracted from confocal microscopy measurements. The diagram shows that for $\xi = 0.011, 0.025, 0.036$ and 0.039 gel states are found for $c_p/c_p^* \geq 0.2$, while for the largest value of $\xi = 0.075$ the percolation line shifts to $c_p/c_p^* = 0.3$. Analysis of samples corresponding to the five investigated values of ξ shows that with increasing size-ratio the structure of the network close to the gelation boundary becomes progressively less compact and less sensitive to the value of ξ.

Fig.4 shows $P(\theta)$ for $c_p/c_p^* = 0.5$ and different values of

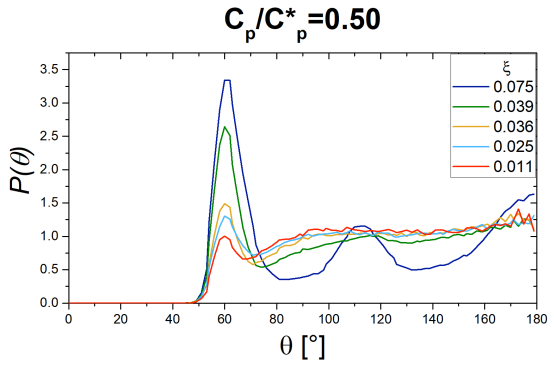

FIG. 4. Angular distribution $P(\theta)$ for $c_p/c_p^* = 0.5$ and different values of the size ratio ξ, as indicated.

ξ. For $\xi = 0.075$ the angular distribution function indicates triangular arrangements typical of compact clusters. Progressively decreasing the value of ξ the peaks become increasingly less pronounced. In particular, the peak at intermediate values of θ progressively broadens and tends to disappear for the smallest values of ξ. $P(\theta)$ for $c_p/c_p^* \geq 0.50$ and $\xi = 0.011$ is similar to that of $c_p/c_p^* \geq 1.00$ and $\xi = 0.039$, characteristic of more open and branched structures. This suggests that for smaller size ratios, i.e. attraction range, the formation of compact structures and heterogeneous networks is inhibited.

This is confirmed when looking at the average number of neighbors $\langle n_b \rangle$ and the corresponding standard deviation σ of the neighbor distribution for different size ratios ξ as a function of c_p/c_p^* (Fig.5). Both, $\langle n_b \rangle$ and σ, are similar for the different ξ values in the fluid phase at small values of c_p/c_p^*. Instead, at intermediate values of c_p/c_p^*, $\langle n_b \rangle$ for $\xi = 0.075$ is almost double the values for $\xi = 0.011$. Values for $\xi = 0.039$ and 0.036 are intermediate, while those for $\xi = 0.025$ are very similar to $\xi = 0.011$. At larger values of c_p/c_p^* values for different ξ become again more comparable. Note also that for the smaller ξ values, samples in which particles form a percolated network only show small variations as a function of c_p/c_p^*. The observed trends thus indicate that for $\xi \lesssim 0.03$ the morphology of aggregates and the network structure become poorly dependent on the potential parameters. We could speculate that $\xi \lesssim 0.03$ is a limiting value for the range of attraction, below which particle bonds are always rigid for the investigated attraction strengths, leading to similar structures independent of ξ and c_p/c_p^*. The fact that the network structure of samples with $\xi = 0.011$ and 0.025 is closely comparable is in good agreement with results of[46], in which the authors claimed that the quantity c_p/c_p^* plays the role of an effective reduced second virial coefficient. Differences in the network and aggregate structure for larger values of ξ might be associated with a stronger interplay between the short-range attraction associated with depletion effects and the weak electrostatic repulsion due to moderate charging of the particles. The standard deviation σ shows a similar trend as $\langle n_b \rangle$ for the different ξ values. This quantity could be linked

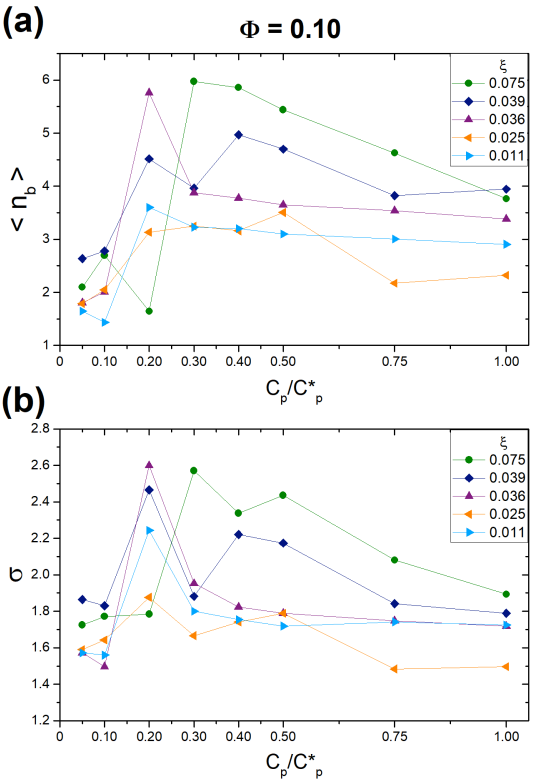

FIG. 5. Average number of neighbors $\langle n_b \rangle$ (a) and standard deviation of the neighbor distribution σ (b) as a function of c_p/c_p^*, for different values of the size ratio ξ, as indicated.

to the heterogeneity of the percolating network and eventually to the mechanism that produces gelation[53]. Systems with the largest attraction ranges are highly heterogeneous at intermediate polymer concentrations as expected for states inside the phase separation region. As the polymer concentration is increased they become more homogeneous. Systems with smaller attraction ranges present a larger heterogeneity only close to the gel transition. The state diagram of Fig.3 reports an indication of the combination of polymer concentration and polymer-colloid size ratio that leads to more elongated or compact/globular aggregate structures, according to the discussion of $P(\theta)$, $\langle n_b \rangle$ and σ presented above, and the results on the fractal dimension presented in the next section.

C. Fractal dimension of clusters: effect of depletant concentration and size

We finally characterized the cluster morphology as a function of polymer concentration and size ratio by determining the cluster radius of gyration and average fractal dimension. The determination of cluster structures was performed according to the connectivity calculations first introduced by Sevick and coworkers[31,54]. Let us recall that when two colloids are separated by a relative distance less than $\sigma + 2\xi$ are assumed

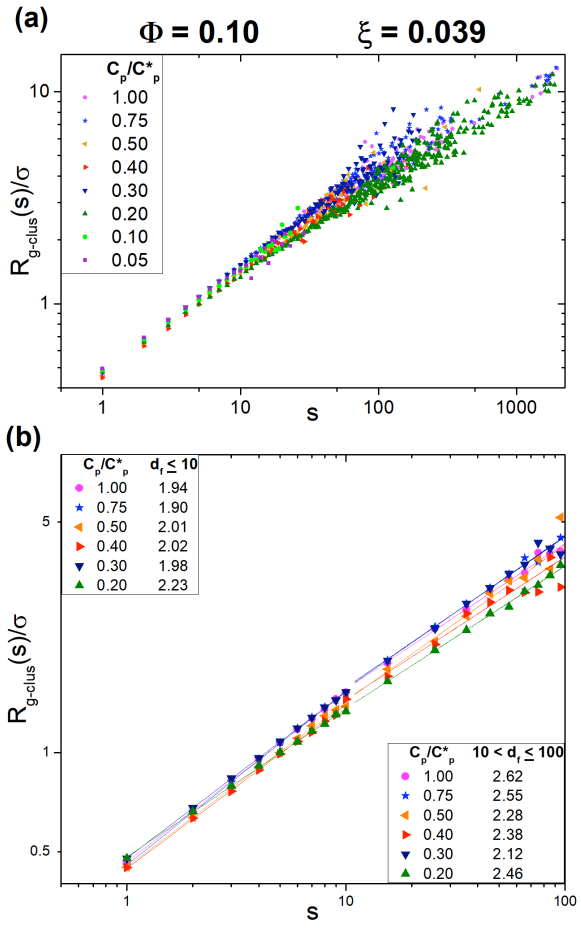

FIG. 6. (a) Cluster radius of gyration R_g as a function of cluster number size s for samples with $\phi = 0.10$, $\xi =$ and different values of c_p/c_p^*, as indicated. (b) Same data shown in separate plots for $s < 10$ (left) and $s > 10$, together with power-law fits. The corresponding fractal dimensions d_f obtained from fits are shown in the legend.

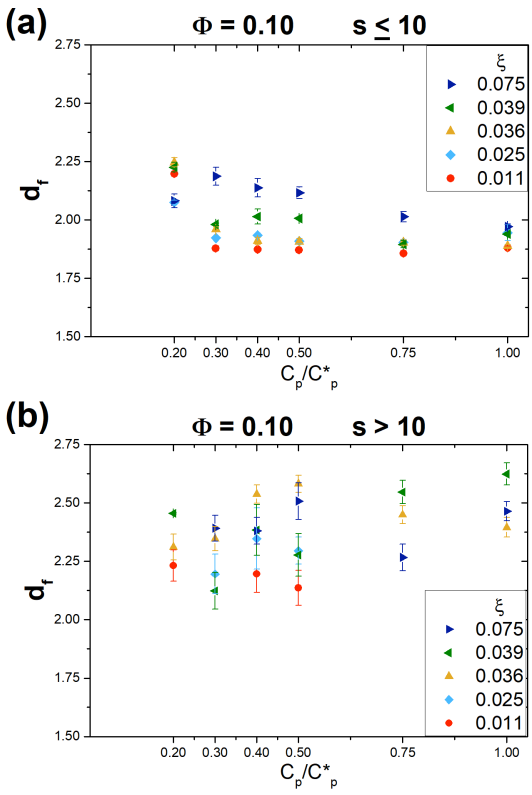

FIG. 7. Cluster radius of gyration R_g as a function of c_p/c_p^* for different values of ξ, as indicated, for $s < 10$ (a) and $s > 10$ (b). cluster number size s for samples with $\phi = 0.10$, $\xi =$ and different values of c_p/c_p^*, as indicated.

to form a bond and, therefore, are part of the same cluster. Once clusters were identified, for a cluster composed of s particles the radius of gyration was determined as[31]:

$$R_g(s) = \left[\frac{1}{s}\sum_{i=1}^{s}(r_i - r_{CM})^2\right]^{1/2}, \qquad (5)$$

where r_i is the coordinate of particle i within the cluster and r_{CM} is the radius of the center of mass of the cluster. The value of $R_g(s)$ is related to the fractal dimension d_f of the clusters, $R_g(s) \sim s^{1/d_f}$.[31,46] We report in Fig.6 exemplary data of $R_g(s)$ as a function of s for samples with $\phi = 0.10$ and $\xi = 0.039$. The curves can be separated in two different regions presenting different dependencies of $R_g(s)$ on s: One region for $s \leq 10$ (small clusters) and one region for $s > 10$ (large clusters). In both regions and for all samples $R_g(s)$ data show a power-law dependence on s. However, the slope, i.e. the power-law exponent, is different. In particular the higher slope observed for $s \leq 10$ corresponds to a smaller d_f.

Additionally, the slope is different depending on the value of c_p/c_p^*. A similar analysis was performed for the other values of ξ. The obtained values of the fractal exponent d_f are reported as a function of c_p/c_p^* in Fig.7, for all values of ξ. The dependence of d_f on c_p/c_p^* for small cluster sizes (Fig.7a), $s < 10$, shows that for $\xi = 0.011$, 0.025 and 0.036 the fractal dimension $d_f \approx 1.9$ is comparable and almost independent of c_p/c_p^* for $c_p/c_p^* > 0.20$. Such value of d_f indicates almost planar elongated structures. Samples with $c_p/c_p^* = 0.2$ present a larger value $d_f \approx 2.25$, corresponding to more compact clusters. For $\xi = 0.039$ $d_f \approx 2.0$ for $c_p/c_p^* = 0.30$, 0.40 and 0.50, while it reaches the value of 1.9 for the largest polymer concentrations. Samples with $\xi = 0.039$ therefore evidence a more pronounced dependence of the aggregate structure on c_p/c_p^*. Such dependence is even more pronounced for samples corresponding to $\xi = 0.075$, which show generally values d_f larger than 2.0 and a decreasing value of d_f with increasing c_p/c_p^* (only for $c_p/c_p^* = 1.00$ d_f approaches the value of 1.9). These observations are consistent with the results of the angular and neighbor distribution functions. For the large clusters with $s > 10$ (Fig.7b) values are generally larger, $2.1 \lesssim d_f \lesssim 2.6$. The value of d_f seems to increase with ξ but no clear dependence on c_p/c_p^* can be evinced due to poorer statistics. The observed trends of d_f are in agreement

with previous results for reversible colloidal aggregation[46].

In summary, for small clusters and very short range attraction the fractal dimension obtained from the analysis of $R_g(s)$ vs. s is almost independent of both depletant concentration and size in percolated networks. For the largest polymer size the results seem not to hold. The fractal dimension is indicative of elongated cluster structures. For larger clusters the result is less clear, due to poorer statistics that lead to larger dispersion of the values of d_f. The fractal dimension although is generally larger and characteristic of more compact clusters.

IV. CONCLUSIONS

We systematically investigated in experiments the structural properties of gel networks formed by colloid-polymer mixtures with moderate colloid volume fraction as a function of attraction strength and range, controlled through the polymer concentration and the polymer-colloid size ratio. We observed that with decreasing polymer-colloid size ratio, i.e. the attraction range, the network structure becomes increasingly similar for corresponding values of the ratio c_p/c_p^*. This is in qualitative agreement with the recent proposal that c_p/c_p^* plays the role of an effective second virial coefficient[46]. We found in addition that for the smallest values of the size-ratio, $\xi \lesssim 0.03$, the structure is also poorly dependent on c_p/c_p^*, i.e. becomes invariant with respect to the potential parameters. In this limit of small ξ values, the structure of the gels is characterized by open cluster structures forming a branched network. This is confirmed by the analysis of the cluster fractal dimension, for which we found two distinct values: one for clusters with less than 10 particles, $d_f \approx 1.9$, and one for clusters with more than 10 particles, $d_f \approx 2.2$. Both values are almost independent of c_p/c_p^* for $\xi \lesssim 0.03$. The different analyses suggest that for moderate volume fraction and sufficiently short attraction range, formation of elongated branched structures is strongly favoured independent of the attraction strength. We could speculate that this finding is connected with the strong rigidity of particle bonds at all tested attraction strengths in the region of small attraction ranges. In addition our findings show qualitative agreement with recent work indicating a stress-free route to colloidal gelation depending on the balance between hydrodynamic and short-range depletion interactions[53]. However, theoretical insight is needed to quantitatively determine and explain the range of parameters for which potential-invariant structures are observed. The different structural evolution observed in particular for the largest size ratio might indicate that a different gelation route is followed by the system in this case.

SUPPLEMENTARY MATERIAL

See supplementary material for additional pair and angular distribution functions corresponding to different values of ξ and c_p/c_p^* and for renderings of the network structures.

AUTHOR'S CONTRIBUTIONS

All authors contributed equally to this work.

ACKNOWLEDGMENTS

We acknowledge financial support from the project "A1-S-9098" funded by Conacyt within the call "Convocatoria de Investigación Básica 2017-2018" and from "Consorzio per lo Sviluppo dei Sistemi a Grande Interfase" (CSGI). R. C-P. also thanks financial support provided by Conacyt (Grants No. 237425 and 287067) and the Marcos Moshinsky Foundation.

DATA AVAILABILITY STATEMENT

The data that support the findings of this study are available from the corresponding author upon reasonable request.

[1] J. Bentley and G. Turner, *Introduction to Paint Chemistry and Principles of Paint Technology, 4th ed.* (Taylor & Francis, London, 1997).
[2] E. Dickinson, "Colloids in food: Ingredients, structure, and stability," Annual Review of Food Science and Technology **6**, 211–233 (2015), pMID: 25422877, https://doi.org/10.1146/annurev-food-022814-015651.
[3] T. F. E. Tadros, *Colloid Stability and Application in Pharmacy*, Vol. 3 (Wiley-VCH Verlag GmbH, 2011).
[4] T. E. Cosgrove, *Colloid Science: Principles, Methods and Applications* (Wiley, 2010).
[5] W. B. Russel, D. A. Saville, and W. R. Schowalter, *Colloidal Dispersions*, Cambridge Monographs on Mechanics (Cambridge University Press, 1989).
[6] Z. Zhang and Y. Liu, "Recent progresses of understanding the viscosity of concentrated protein solutions," Current Opinion in Chemical Engineering **16**, 48 – 55 (2017), nanotechnology / Separation Engineering.
[7] A. Aguzzi and T. O'Connor, "Protein aggregation diseases: pathogenicity and therapeutic perspectives," Nature Reviews Drug Discovery **9**, 237–248 (2010).
[8] Y. Shin and C. P. Brangwynne, "Liquid phase condensation in cell physiology and disease," Science **357** (2017), 10.1126/science.aaf4382, https://science.sciencemag.org/content/357/6357/eaaf4382.full.pdf.
[9] P. Germain and S. Amokrane, "Equilibrium and glassy states of the asakura-oosawa and binary hard sphere mixtures: Effective fluid approach," Phys. Rev. E **76**, 031401 (2007).
[10] K. Binder, P. Virnau, and A. Statt, "Perspective: The asakura oosawa model: A colloid prototype for bulk and interfacial phase behavior," The Journal of Chemical Physics **141**, 140901 (2014), https://doi.org/10.1063/1.4896943.
[11] P. N. Pusey, "Liquids, freezing and glass transition," (Elsevier, 1991) pp. 764–942.
[12] W. C. K. Poon, S. M. Ilett, and P. N. Pusey, "Phase behaviour of colloid-polymer mixtures," Il Nuovo Cimento D **16**, 1127–1139 (1994).
[13] S. M. Ilett, A. Orrock, W. C. K. Poon, and P. N. Pusey, "Phase behavior of a model colloid-polymer mixture," Phys. Rev. E **51**, 1344–1352 (1995).
[14] S. Shah, Y.-L. Chen, S. Ramakrishnan, K. Schweizer, and C. Zukoski, "Microstructure of dense colloid-polymer suspensions and gels," J. Phys. Condens. Matter **15**, 4751–4778 (2003).
[15] V. Trappe and P. Sandkühler, "Colloidal gels–low-density disordered solid-like states," Current Opinion in Colloid & Interface Science **8**, 494 – 500 (2004).
[16] H. Sedgwick, S. U. Egelhaaf, and W. C. K. Poon, "Clusters and gels in systems of sticky particles," Journal of Physics: Condensed Matter **16**, S4913–S4922 (2004).
[17] C. J. Dibble, M. Kogan, and M. J. Solomon, "Structure and dynamics of colloidal depletion gels: Coincidence of transitions and heterogeneity," Phys. Rev. E **74**, 041403 (2006).

[18] E. Zaccarelli, "Colloidal gels: equilibrium and non-equilibrium routes," Journal of Physics: Condensed Matter **19**, 323101 (2007).

[19] A. Kozina, P. Díaz-Leyva, C. Friedrich, and E. Bartsch, "Structural and dynamical evolution of colloid-polymer mixtures on crossing glass and gel transition as seen by optical microrheology and mechanical bulk rheology," Soft Matter **8**, 1033–1046 (2012).

[20] M. E. Helgeson, Y. Gao, S. E. Moran, J. Lee, M. Godfrin, A. Tripathi, A. Bose, and P. S. Doyle, "Homogeneous percolation versus arrested phase separation in attractively-driven nanoemulsion colloidal gels," Soft Matter **10**, 3122–3133 (2014).

[21] E. Del Gado, D. Fiocco, G. Foffi, S. Manley, V. Trappe, and A. Zaccone, "Colloidal gelation," in *Fluids, Colloids and Soft Materials* (John Wiley & Sons, Ltd, 2016) Chap. 14, pp. 279–291, https://onlinelibrary.wiley.com/doi/pdf/10.1002/9781119220510.ch14.

[22] S. Asakura and F. Oosawa, "Interaction between particles suspended in solutions of macromolecules," Journal of Polymer Science **33**, 183–192 (1958), https://onlinelibrary.wiley.com/doi/pdf/10.1002/pol.1958.1203312618.

[23] P. J. Lu, E. Zaccarelli, F. Ciulla, A. B. Schofield, F. Sciortino, and D. A. Weitz, "Gelation of particles with short-range attraction," Nature **453**, 499–503 (2008).

[24] J. C. Conrad, H. M. Wyss, V. Trappe, S. Manley, K. Miyazaki, L. J. Kaufman, A. B. Schofield, D. R. Reichman, and D. A. Weitz, "Arrested fluid-fluid phase separation in depletion systems: Implications of the characteristic length on gel formation and rheology," Journal of Rheology **54**, 421–438 (2010), https://doi.org/10.1122/1.3314295.

[25] N. Park and J. Conrad, "Phase behavior of colloid-polymer depletion mixtures with unary or binary depletants," Soft Matter **13**, 2781–2792 (2017).

[26] A. González García and R. Tuinier, "Tuning the phase diagram of colloid-polymer mixtures via yukawa interactions," Phys. Rev. E **94**, 062607 (2016).

[27] N. Kovalchuk, V. Starov, P. Langston, and N. Jilal, "Formation of stable clusters in colloidal suspensions," Adv. Colloid Interface Sci. **147**, 144 (2009).

[28] C. L. Klix, C. P. Royall, and H. Tanaka, "Structural and dynamical features of multiple metastable glassy states in a colloidal system with competing interactions," Phys. Rev. Lett. **104**, 165702 (2010).

[29] P. D. Godfrin, N. E. Valadez-Perez, R. Castañeda-Priego, N. J. Wagner, and Y. Liu, "Generalized phase behavior of cluster formation in colloidal dispersions with competing interactions," Soft Matter **10**, 5061 (2014).

[30] M. B. Sweatman, R. Fartaria, and L. Lue, "Cluster formation in fluids with competing short-range and long-range interactions," The Journal of Chemical Physics **140**, 124508 (2014), https://doi.org/10.1063/1.4869109.

[31] N. E. Valadez-Pérez, R. Castañeda Priego, and Y. Liu, "Percolation in colloidal systems with competing interactions: the role of long-range repulsion," RSC Adv. **3**, 25110 (2013).

[32] M. Kohl, R. F. Capellmann, M. Laurati, S. U. Egelhaaf, and M. Schmiedeberg, "Directed percolation identified as equilibrium pre-transition towards non-equilibrium arrested gel states," Nat. Commun. **7**, 11817 (2016).

[33] Y. Liu and Y. Xi, "Colloidal systems with a short-range attraction and long-range repulsion: Phase diagrams, structures, and dynamics," Current Opinion in Colloid & Interface Science **39**, 123 – 136 (2019), special Topic Section: Outstanding Young Researchers in Colloid and Interface Science.

[34] A. I. Campbell, V. J. Anderson, J. S. van Duijneveldt, and P. Bartlett, "Dynamical arrest in attractive colloids: The effect of long-range repulsion," Phys. Rev. Lett. **94**, 208301 (2005).

[35] P. D. Godfrin, R. Castañeda-Priego, Y. Liu, and N. J. Wagner, "Intermediate range order and structure in colloidal dispersions with competing interactions," The Journal of Chemical Physics **139**, 154904 (2013), https://doi.org/10.1063/1.4824487.

[36] R. F. Capellmann, N. E. Valadez-Pérez, B. Simon, S. U. Egelhaaf, M. Laurati, and R. Castañeda-Priego, "Structure of colloidal gels at intermediate concentrations: the role of competing interactions," Soft Matter **12**, 9303–9313 (2016).

[37] J. Ruiz-Franco, F. Camerin, N. Gnan, and E. Zaccarelli, "Tuning the rheological behavior of colloidal gels through competing interactions," Phys. Rev. Materials **4**, 045601 (2020).

[38] J. E. Verweij, F. A. M. Leermakers, J. Sprakel, and J. van der Gucht, "Plasticity in colloidal gel strands," Soft Matter **15**, 6447–6454 (2019).

[39] P. J. Lu, J. C. Conrad, H. M. Wyss, A. B. Schofield, and D. A. Weitz, "Fluids of clusters in attractive colloids," Phys. Rev. Lett. **96**, 028306 (2006).

[40] A. Imperio and L. Reatto, "Microphase morphology in two-dimensional fluids under lateral confinement," Phys. Rev. E **76**, 040402 (2007).

[41] I. Zhang, C. Royall, M. Faers, and P. Bartlett, "Phase separation dynamics in colloid-polymer mixtures: The effect of interaction range," Soft Matter **9**, 2076–2084 (2013).

[42] N. I. Lebovka, "Polyelectrolyte complexes in the dispersed and solid state i: Principles and theory," (Springer, Berlin, Heidelberg, 2013) pp. 57–96.

[43] S. Haddadi, M. Skepö, P. Jannasch, S. Manner, and J. Forsman, "Building polymer-like clusters from colloidal particles with isotropic interactions, in aqueous solution," Journal of Colloid and Interface Science **581**, 669 – 681 (2021).

[44] F. Sciortino, P. Tartaglia, and E. Zaccarelli, "One-dimensional cluster growth and branching gels in colloidal systems with short-range depletion attraction and screened electrostatic repulsion," *The Journal of Physical Chemistry B*, The Journal of Physical Chemistry B **109**, 21942–21953 (2005).

[45] T. Ohtsuka, C. P. Royall, and H. Tanaka, "Local structure and dynamics in colloidal fluids and gels," Europhys. Lett. **84**, 46002 (2008).

[46] N. E. Valadez-Pérez, Y. Liu, and R. Castañeda Priego, "Reversible aggregation and colloidal cluster morphology: The importance of the extended law of corresponding states," Phys. Rev. Lett. **120**, 248004 (2018).

[47] G. C. Berry, "Thermodynamic and conformational properties of polystyrene. i. light-scattering studies on dilute solutions of linear polystyrenes," The Journal of Chemical Physics **44**, 4550–4564 (1966), https://doi.org/10.1063/1.1726673.

[48] C. P. Royall, M. E. Leunissen, A.-P. Hynninen, M. Dijkstra, and A. van Blaaderen, "Re-entrant melting and freezing in a model system of charged colloids," The Journal of Chemical Physics **124**, 244706 (2006), https://doi.org/10.1063/1.2189850.

[49] J. Dobnikar, R. Castañeda-Priego, H. H. von Grünberg, and E. Trizac, "Testing the relevance of effective interaction potentials between highly-charged colloids in suspension," New Journal of Physics **8**, 277–277 (2006).

[50] C. P. Royall, W. C. K. Poon, and E. R. Weeks, "In search of colloidal hard spheres," Soft Matter **9**, 17–27 (2013).

[51] J. C. Crocker and D. G. Grier, "Methods of digital video microscopy for colloidal studies," Journal of Colloid and Interface Science **179**, 298 – 310 (1996).

[52] Y. Gao and M. Kilfoil, "Experimental determination of order in non-equilibrium solids using colloidal gels," Journal of Physics: Condensed Matter **16**, S5191–S5202 (2004).

[53] H. Tsurusawa, S. Arai, and H. Tanaka, "A unique route of colloidal phase separation yields stress-free gels," Science Advances **6** (2020), 10.1126/sciadv.abb8107, https://advances.sciencemag.org/content/6/41/eabb8107.full.pdf.

[54] E. M. Sevick, P. A. Monson, and J. M. Ottino, "Monte carlo calculations of cluster statistics in continuum models of composite morphology," J. Chem. Phys. **88**, 1198 (1998).